OFFICE OF NAVAL RESEARCH

WORK ORDER NO. N00014-91-WX-24203

R&T Code 4134057

Technical Report No. 1

DECOMPOSITION MECHANISMS OF ANTIMONY SOURCE COMPOUNDS FOR ORGANOMETALLIC VAPOR-PHASE EPITAXY

C. A. Larsen, R. W. Gedridge, Jr., S. H. Li, G. B. Stringfellow

Prepared for Publication in

MATERIALS RESEARCH SOCIETY SYMPOSIUM PROCEEDINGS

December 1990

Research Department
Chemistry Division
Naval Weapons Center
China Lake, CA 93555

DECOMPOSITION MECHANISMS OF ANTIMONY SOURCE COMPOUNDS FOR ORGANOMETALLIC VAPOR-PHASE EPITAXY

Cory A. Larsen,*§ Robert W. Gedridge, Jr.,** Shin Hwa Li,* Gerald B. Stringfellow*

*Dept. of Material Science and Engineering, University of Utah, Salt Lake City, UT 84112
**Chemistry Division, Research Dept., Naval Weapons Center, China Lake, CA 93555
§Current Address: Dept. of Electronic Materials Engineering, Australian National University, Canberra, ACT, 2601

ABSTRACT

The decompositions of tertiary stibines (R_3Sb, R = methyl, vinyl, isopropyl) were studied in an atmospheric pressure flow tube reactor, using D_2 and He as carrier gases. D_2 was used to isotopically label the byproducts in order to elucidate the pyrolysis mechanism. The exhaust products were analyzed by a time-of-flight mass spectrometer. The decomposition of these tertiary stibines in the presence of group III precursors was studied in order to simulate the conditions of organometallic vapor phase epitaxial growth. A comparison between the pyrolysis temperatures, decomposition mechanisms, and surface area effects of these Sb source compounds is presented.

INTRODUCTION

Organometallic vapor phase epitaxy (OMVPE) is a high throughput technique for the production of high quality III/V semiconductor materials and complex structures from organometallic precursors. This technique has been used to produce Sb-containing metastable materials such as GaInAsSb [1], GaPSb [2], InPSb [3], and GaAsSb [4] which have never been produced by any other technique.

$InAs_{1-x}Sb_x$ which can also be grown by OMVPE [5], has the smallest band gap (x = 0.6, E_g ≈ 0.1 eV at 300 K) of any of the III/V semiconductor materials and this has attracted interest for infrared detection in the 8-12 μm spectral range. The cutoff wavelength at 77 K for $InAs_{1-x}Sb_x$ (x = 0.6) is ≈ 9 μm. Further reduction of the band gap is required to extend the cutoff wavelength and can occur if the crystal lattice is dilated with the heavier Group V element Bi. $InAs_{1-x-y}Sb_yBi_x$ [6, 7] and $InSb_{1-x}Bi_x$ [6] have been grown by OMVPE using trimethylantimony (TMSb). Bi concentrations higher than 2 atom %, as well as growth temperatures above 400 ℃, resulted in poor film morphology. Growth temperatures lower than 400 ℃ resulted in significant problems due to the incomplete pyrolysis of TMSb. In order to minimize the tendency of the Bi to phase separate and to limit the diffusion in these alloys, alternative Sb precursors having lower pyrolysis temperatures than TMSb need to be investigated.

While SbH_3 gas has been used in the OMVPE growth of InSb at temperatures as low as 300 ℃ [8], it is unstable at room temperature and therefore was generated at the point of use. Higher homologues such as $(CH_3)SbH_2$ and $(CH_3)_2SbH$ are also unstable at room temperature [9]. Trivinylantimony (TVSb) was investigated since it is a stable tertiary stibine with an acceptable vapor pressure (≈ 8.5 Torr at room temperature) [10]. Another motivation for studying TVSb is that tetravinyltellurium is less stable than tetramethyltellurium [11]. This contrasts the predicted higher activation energy for vinyl radical formation in comparison to methyl radical formation [12] and studies suggested that tetravinyltellurium decomposition may occur by a non-coupling reductive elimination pathway [13]. Triisopropylantimony (TIPSb) was investigated in spite of its low vapor pressure (≈ 0.4 Torr at room temperature) since the activation energy for isopropyl radical formation is less than that for methyl or vinyl radical formation.

EXPERIMENTAL

The trimethylantimony, $(CH_3)_3Sb$, (TMSb) was purchased from Alfa. Trivinylantimony, $(CH_2=CH)_3Sb$, (TVSb) [10] and triisopropylantimony, $((CH_3)_2CH)_3Sb$, (TIPSb) [14] were prepared by reaction of $SbCl_3$ with 3 equiv of the corresponding Grignard reagent according to the literature. These colorless source compounds were purified by multiple vacuum distillation under Ar. The D_2 used was research grade from Air Products and Chemicals, Inc.

The atmospheric pressure flow tube reactor used in these experiments has been described in detail elsewhere [15]. The carrier gases pass through mass flow controllers, then through stainless steel bubblers containing the reactants. The flow rate for most experiments was 40 sccm. The organoantimony compound concentration for most experiments was about 1%, although it was 20 times lower for TIPSb due to the low vapor pressure. In each case, the reactor was conditioned by heating the tube to a temperature near which 50 % of the Sb compound decomposed. For some runs the tube was packed with SiO_2 chips to increase the surface area approximately 24 times. The flow rates were correspondingly adjusted to give the same residence times as for the unpacked runs. The exhaust gases were sampled continuously via a variable leak connected to a CVC 2000 time-of-flight mass spectrometer.

RESULTS AND DISCUSSION

TMSb, TVSb, and TIPSb were pyrolyzed in He and D_2 and the percent decomposition for each as a function of temperature is shown in Figure 1.

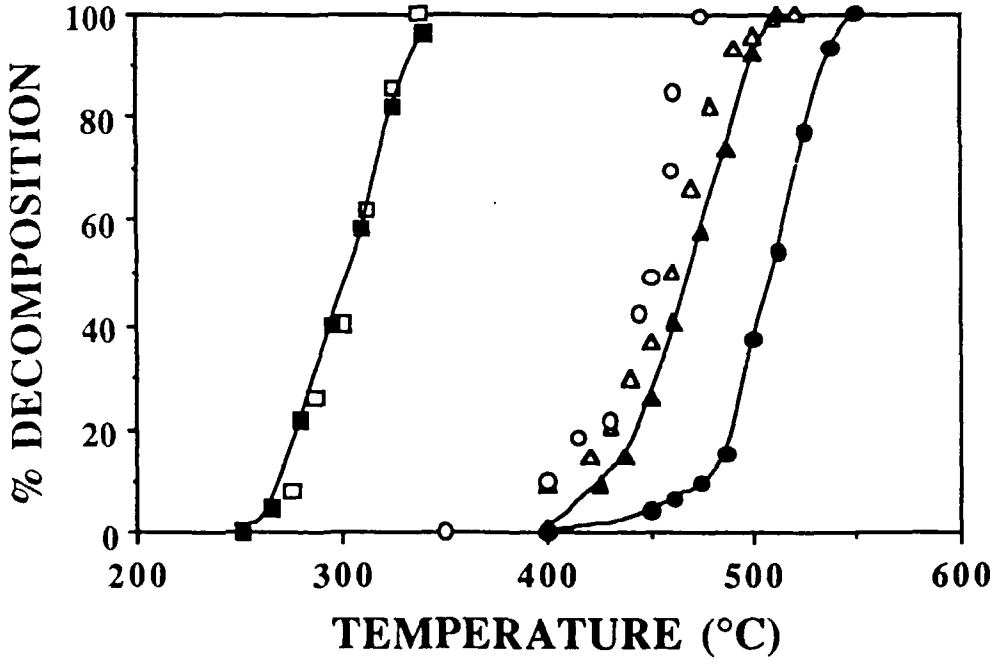

Figure 1. Pyrolysis of TMSb in He (●) and D_2 (○), TVSb in He (▲) and D_2 (△), and TIPSb in He (■) and D_2 (❑).

The decomposition rate of TIPSb is independent of the ambient gas. The slight difference in temperature ($\Delta T \approx 10$ °C) between the decomposition of TVSb in He and D_2 is close to the error limits of the system. In contrast, TMSb pyrolyzes significantly lower (> 50 °C) in D_2 than in He. The increase in the decomposition rate of TMSb in D_2 is due to the attack on the parent molecule

by D atoms [16]. Apparently, D atoms do not have an effect on the pyrolysis of TVSb [17] or TIPSb.

The similarity of the decomposition rates of TVSb and TIPSb in He and D_2 indirectly implies the reaction is unimolecular in both. Assuming the overall decomposition processes for both TVSb and TIPSb are first order, plots of -ln[P/Po] versus t from the integrated rate law for a first order reaction (eq 1), resulted in straight lines passing approximately through the origin.

$$-\ln[P/Po] = kt \qquad (1)$$

The first order assumption is nearly correct. Therefore, pyrolysis data in He for TVSb and TIPSb can be used to calculate P/Po for the entire temperature range, and the results were used to construct Arrhenius plots shown in Figure 2. The resulting rate constants for TVSb and TIPSb derived from the Arrhenius plots are shown in eq 2 and 3, respectively.

$$\log k\ (s^{-1}) = 13.9 - 49.0\ (\text{kcal/mol})/2.303RT \qquad (2)$$
$$\log k\ (s^{-1}) = 11.0 - 30.8\ (\text{kcal/mol})/2.303RT \qquad (3)$$

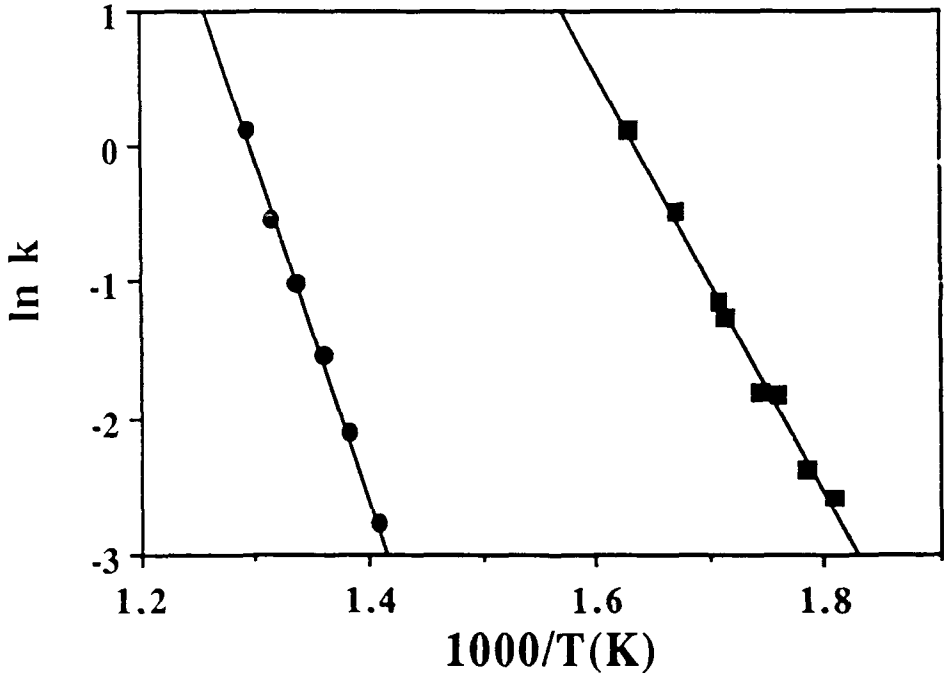

Figure 2. Arrhenius plots for TVSb (●) and TIPSb (■).

The activation energy for TVSb decomposition derived from eq 2 (49.0 kcal/mol) is less than the reported Sb-C bond energy for TMSb (55.9 kcal/mol) [18]. The activation energy for TIPSb decomposition derived from eq 3 (30.8 kcal/mol), which may represent the Sb-C bond strength in TIPSb, is substantially lower than for TMSb and TVSb.

The surface area of the reactor was increased to determine the extent of heterogeneous pyrolysis reactions. As shown in Figure 3, a 24-fold increase in surface area did not affect the decomposition temperatures of TVSb in D_2. However, small surface area effects were observed for the pyrolysis of TMSb in H_2 and TIPSb in D_2.

TMSb pyrolysis [16] in He produces mainly C_2H_6, CH_4, and C_3H_8. C_2H_4 and C_3H_6 were not identified due to the potential overlapping mass spectral peaks from other byproducts. These products can be accounted for by normal free-radical processes. C_2H_6 arises from CH_3 radical recombination (reaction 4). C_3H_8 and CH_4 are produced according to reactions 5 and 6.

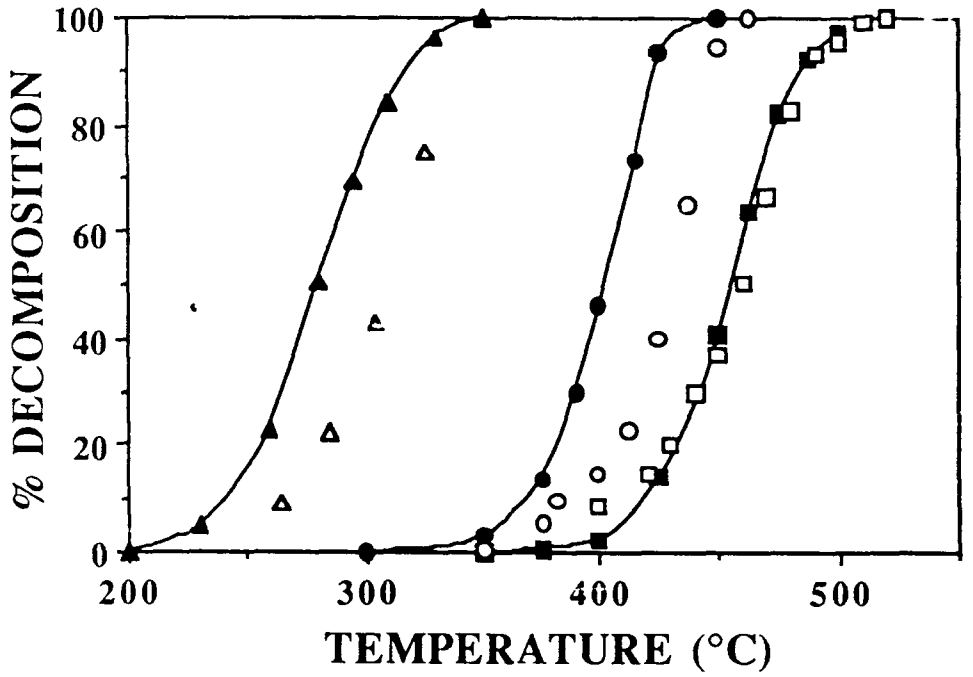

Figure 3. Pyrolysis of TMSb in H_2 with low (○) and high (●) surface area, TVSb with low (❑) and high (■) surface area, and TIPSb with low (Δ) and high (▲) surface area.

$$2CH_3 \rightarrow C_2H_6 \quad (4)$$

$$CH_3 + C_2H_6 \rightarrow CH_4 + C_2H_5 \quad (5)$$

$$CH_3 + C_2H_5 \rightarrow C_3H_8 \quad (6)$$

CH_4 could arise from reaction 5 and other H abstraction steps. The major product from the pyrolysis of TMSb in D_2 is CH_3D with a trace of C_2H_6. No CH_4 or deuterated Sb species were detected. This suggests that methyl radical attack on the TMSb parent molecule or its decomposition products to abstract H atoms is unimportant. The addition of azomethane $(CH_3N)_2$ as a "clean" source of methyl radicals retards the TMSb decomposition slightly. This supports a reversible step in TMSb pyrolysis (reaction 7) that was previously reported [18]. Overall, homolytic fission of the Sb-C bonds in TMSb followed by normal free-radical reactions appears to describe the pyrolysis of TMSb under these conditions.

$$(CH_3)_3Sb \leftrightarrow (CH_3)_2Sb + CH_3 \quad (7)$$

Two alternative mechanisms for TVSb pyrolysis are proposed. The first is simple Sb-C bond homolysis of TVSb to produce vinyl radicals. The expected subsequent radical reactions are:

$$CH_2{=}CH + D_2 \rightarrow CH_2{=}CHD + D \quad (8)$$

$$CH_2{=}CH + D \rightarrow CH_2{=}CHD \quad (9)$$

$$2\ CH_2{=}CH \rightarrow CH_2{=}CH\text{-}CH{=}CH_2 \quad (10)$$

$$2\ CH_2{=}CH \rightarrow CH_2{=}CH_2 + HC{\equiv}CH \quad (11)$$

The other possible mechanism for TVSb pyrolysis involves an Sb-centered reductive elimination pathway.

$$(CH_2{=}CH)_3Sb \rightarrow (CH_2{=}CH)Sb + CH_2{=}CH\text{-}CH{=}CH_2 \quad (12)$$

$$(CH_2{=}CH)Sb \rightarrow CH_2{=}CH + Sb \quad (13)$$

$$(CH_2{=}CH)Sb + D_2 \rightarrow (CH_2{=}CH)SbD_2 \quad (14)$$

$$(CH_2{=}CH)SbD_2 \rightarrow CH_2{=}CHD + SbD \quad (15)$$

$$SbD \rightarrow Sb + D \quad (16)$$

This route would generate $CH_2{=}CH\text{-}CH{=}CH_2$ in the first step by coupling two vinyl groups (reaction 12). There are several reasons for suspecting this to be the operative mechanism. First, the activation energy for TVSb decomposition (eq 2) is less than that found for scission of the Sb-CH_3 bond in TMSb [16, 18]. If Sb-C bond homolysis occurs, one would expect the Sb-vinyl bond strength to be higher than the Sb-methyl bond strength. Second, TVSb decomposes 50 °C lower in temperature than TMSb in He. These observations are contrary to the predicted higher activation energy for vinyl radical formation than for methyl radical formation. This implies that the rate determining step in TVSb decomposition may not involve Sb-C bond homolysis to form vinyl radicals. However, one cannot rule out the possibility of the $(CH_2{=}CH)Sb$ intermediate decomposing to $CH_2{=}CH$ radicals (reaction 13).

The unambiguous identification of the unsaturated hydrocarbon byproducts from TVSb pyrolysis is difficult. In He, TVSb pyrolysis results in $CH_2{=}CH\text{-}CH{=}CH_2$ as the major byproduct. A trace of $CH_2{=}CH\text{-}CH{=}CH\text{-}CH{=}CH_2$, from oligomerization reactions involving alkene byproducts, was also observed. In D_2, the only products observed were $CH_2{=}CHD$ and $CH_2{=}CH\text{-}CH{=}CH_2$. $HC{\equiv}CH$ and deuterated Sb species were not detected, indicating that the non-coupling reductive elimination from the tetravinyltellurium study [13] was not operative for this molecule. If vinyl radicals are present, they should disproportionate as well as recombine (reaction 10 and 11). The non-production of vinyl radicals is further attested by an experiment in which a high concentration of C_7D_8 (C_7D_8/TVSb = 5/1) was added to TVSb in He. In this case, no $CH_2{=}CHD$ was found. This implies vinyl radicals are not present or C_7D_8 is not an effective vinyl radical trapping reagent. It was not possible to detect $CH_2{=}CH_2$ concentration due to the overlap of its spectrum with fragments from other molecules.

The byproducts identified from TIPSb pyrolysis in He were C_3H_6, C_3H_8, and C_6H_{14}. These products can be accounted for from normal free-radical processes. Isopropyl radicals can undergo a recombination reaction (eq 17) or disproportionation reaction (eq 18).

$$2\,C_3H_7 \rightarrow C_6H_{14} \quad (17)$$

$$2\,C_3H_7 \rightarrow C_3H_6 + C_3H_8 \quad (18)$$

$$C_3H_7 + D_2 \rightarrow C_3H_7D + D \quad (19)$$

In addition to the products observed in He, C_3H_7D was observed from TIPSb pyrolysis in D_2. This can be attributed to isopropyl radicals reacting with the D_2 ambient (reaction 19). No deuterated Sb intermediates were observed. Free-radical trapping experiments were done with 1,4-cyclohexadiene (C_6H_8) and TIPSb. The only by-product observed from TIPSb pyrolysis in He and D_2 was C_3H_8. C_6H_{14} or C_3H_7D were not produced when C_6H_8 was added. This indicates that C_6H_8 is an effective isopropyl radical scavenger. Overall, the pyrolysis of TIPSb occurs by homolytic fission of the Sb-C bonds to form isopropyl radicals.

The decomposition of TMSb and TVSb in the presence of group III precursors was studied in order to simulate the conditions of OMVPE growth. The addition of trimethylindium (TMIn) to

TMSb results in the accelerated decomposition of TMSb ($\Delta T \approx 50$ °C) but TMIn decomposition is retarded. The decomposition reactions for the TMIn/TMSb mixture are largely the same as for the individual constituents. The first step in TMIn pyrolysis results is the simultaneous loss of two methyl radicals [19]. These methyl radicals react with the D_2 ambient to form D atoms. Further studies indicate that the D atoms then attack TMIn [20]. However, the D atoms from TMIn pyrolysis are also removed by attacking TMSb [16]. The net effect of the competition for the D radicals during pyrolysis of the TMIn/TMSb mixtures is the retardation of TMIn pyrolysis and simultaneous enhancement of TMSb pyrolysis.

While the addition of trimethylgallium (TMGa) to TVSb results in an accelerated decomposition of TVSb ($\Delta T \approx 50$ °C), TMGa decomposition is retarded. Although D atoms do not appear to attack TVSb, the addition of $(CH_3N)_2$ as a methyl radical source significantly enhances the pyrolysis of TVSb ($\Delta T \approx 100$ °C). This suggests that methyl radicals attack TVSb. The addition of TMGa apparently enhances the pyrolysis of TVSb by providing methyl radicals. However, the methyl radicals also increase the rate of TMGa pyrolysis [21]. Since they are removed by attacking TVSb, the net effect in TMGa/TVSb mixtures is the retardation of TMGa pyrolysis and simultaneous enhancement of TVSb pyrolysis.

ACKNOWLEDGMENTS

We would like to acknowledge financial support from the Office of Naval Research, the Office of Naval Technology, and the Air Force Office of Scientific Research.

REFERENCES

1. M.J. Cherng, H.R. Jen, C.A. Larsen, G.B. Stringfellow, H. Lundt, P.C. Taylor, *J. Cryst. Growth* 77, 408 (1986).
2. M.J. Jou, Y.T. Cherng, H.R. Jen, G.B. Stringfellow, *Appl. Phys. Lett.* 52, 549 (1988).
3. M.J. Jou, Y.T. Cherng, G.B. Stringfellow, *J. Appl. Phys.* 64, 1472 (1988).
4. M.J. Cherng, Y.T. Cherng, H.R. Jen, P. Harper, R.M. Cohen, G.B. Stringfellow, *J. Electron. Mater.* 15, 79 (1986).
5. (a) G. Nataf, C. Verie, *J. Cryst. Growth* 55, 87 (1981). (b) P.K. Chiang, S.M. Bediar, *Appl. Phys. Lett.* 46, 383 (1985). (c) R.M. Biefeld, *J. Cryst. Growth* 75, 255 (1986).
6. T.P. Humphreys, P.K. Chiang, S.M. Bediar, N.R. Parikh, *Appl. Phys. Lett.* 53, 142 (1988).
7. K.Y Ma, D.H. Fang, R.M. Jaw, R.M. Cohen, G.B. Stringfellow, W.P. Kosar, D.W. Brown, *Appl. Phys. Lett.* 55, 2420 (1989).
8. O. Sugiura, H. Kameda, K. Shiina, M. Matsumura, *J. Electron. Mater.* 17, 11 (1988).
9. (a) G.G. Devyatykh, V.M. Kedyarkin, A.D. Zorin, *Russ. J. Inorg. Chem.* 14, 1055 (1969). (b) A.B. Burg, L.R. Grant, *J. Am. Chem. Soc.* 81, 1 (1959).
10. L Maier, D. Seyferth, F.G.A. Stone, E.G. Rochow, *J. Am. Chem. Soc.* 79, 5884 (1957).
11. R.W. Gedridge, Jr., D.C. Harris, K.T. Higa, R.A. Nissan, *Organometallics* 8, 2817 (1989).
12. *Handbook of Chemistry and Physics*, ed. R.C. Weast (CRC, Boca Raton, FL, 1988), 70th ed., pp F206-207.
13. R.W. Gedridge, Jr., K.T. Higa, R.A. Nissan, *Organometallics* (in press).
14. H.J. Breunig, W. Kanig, *J. Organomet. Chem.* 186, C5 (1980).
15. N.I. Buchan, C.A. Larsen, G.B. Stringfellow, *Appl. Phys. Lett.* 51, 1024 (1987).
16. C.A. Larsen, S.H. Li, G.B. Stringfellow, *Chem. Mater.* (in press).
17. C.A. Larsen, R.W. Gedridge, Jr., G.B. Stringfellow, *Chem. Mater.* (in press).
18. S.J.C. Price, J.P. Richard, *Can. J. Chem.* 50, 966 (1972).
19. M.G. Jacko, S.J. Price, *Can. J. Chem.* 42, 1198 (1964).
20. N.I. Buchan, C.A. Larsen, G.B. Stringfellow, *J. Cryst. Growth* 92, 591 (1988).
21. C.A. Larsen, N.I. Buchan, S.H. Li, G.B. Stringfellow, *J. Cryst. Growth* 102, 103 (1990).

TECHNICAL REPORT DISTRIBUTION LIST - GENERAL

Office of Naval Research (2)*
Chemistry Division, Code 1113
800 North Quincy Street
Arlington, Virginia 22217-5000

Dr. James S. Murday (1)
Chemistry Division, Code 6100
Naval Research Laboratory
Washington, D.C. 20375-5000

Dr. Robert Green, Director (1)
Chemistry Division, Code 385
Naval Weapons Center
China Lake, CA 93555-6001

Dr. Eugene C. Fischer (1)
Code 2840
David Taylor Research Center
Annapolis, MD 21402-5067

Dr. Elek Lindner (1)
Naval Ocean Systems Center
Code 52
San Diego, CA 92152-5000

Commanding Officer (1)
Naval Weapons Support Center
Dr. Bernard E. Douda
Crane, Indiana 47522-5050

Dr. Richard W. Drisko (1)
Naval Civil Engineering
Laboratory
Code L52
Port Hueneme, CA 93043

Dr. Harold H. Singerman (1)
David Taylor Research Center
Code 283
Annapolis, MD 21402-5067

Chief of Naval Research (1)
Special Assistant for Marine
Corps Matters
Code 00MC
800 North Quincy Street
Arlington, VA 22217-5000

Defense Technical Information
Center (2)
Building 5, Cameron Station
Alexandria, VA 22314

* Number of copies to forward